

# Optical conductivity and charge ordering in $\text{Na}_x\text{CoO}_2$

S. Lupi, M. Ortolani, L. Baldassarre, and P. Calvani

"Coherencia"-INFN and Dipartimento di Fisica, Università di Roma La Sapienza, Piazzale Aldo Moro 2, I-00185 Roma, Italy

D. Prabhakaran and A. T. Boothroyd

Department of Physics, Oxford University, Oxford, OX1 3PU, United Kingdom

(Received 25 January 2005; revised manuscript received 17 March 2005; published 29 July 2005)

The infrared conductivity  $\sigma(\omega)$  of  $\text{Na}_x\text{CoO}_2$  is studied as a function of doping and temperature for  $0.5 \leq x \leq 1$ . A far-infrared peak (FIP) in  $\sigma(\omega)$ , which coexists with a small Drude contribution, indicates charge localization in the  $\text{CoO}_2$  layers. Long-range ordering at  $x=0.5$  is confirmed to create a far-infrared gap, in addition to the FIP. At low  $T$  and high incommensurate  $x$  values, in correspondence with the reported formation of a spin-density wave, the FIP abruptly shifts to higher energy, indicating a deepening of the localizing potential. An analysis of the in-plane  $E_{1u}$  phonon lifetime shows that  $\text{Na}^+$  ions lattice is "frozen in" at any  $T < 295$  K for commensurate  $x$  and at  $T \leq 150$  K for incommensurate  $x$ . A comparison with the behavior of the FIP suggests that the  $\text{Na}^+$  "freezing" induces carrier localization only for low charge density and high  $\text{Na}^+$  concentration.

DOI: [10.1103/PhysRevB.72.024550](https://doi.org/10.1103/PhysRevB.72.024550)

PACS number(s): 74.25.Gz, 74.72.-h, 74.25.Kc

## I. INTRODUCTION

In low-dimensional, correlated electron systems, Coulomb, magnetic, and charge-lattice interactions are known to produce competitive ground states. For example, in cuprates at low temperature one may observe either unconventional superconductivity or charge-spin ordering, or both. The recent discovery<sup>1</sup> of the "wet" superconductor  $\text{Na}_x\text{CoO}_2 \cdot y\text{H}_2\text{O}$  added a new oxide to the list of those which exhibit such intriguing properties.

The anhydrous parent compound of the superconducting cobaltates,  $\text{Na}_x\text{CoO}_2$  (NCO), has a hexagonal crystal structure ( $P6_3/mmc$ ). Its  $ab$  planes are formed by  $\text{CoO}_2$  layers separated by  $\text{Na}^+$  ions. Such ions are highly mobile among three different lattice sites: in Na(1) the  $\text{Na}^+$  ion is placed at  $(0, 0, 1/4)$ , above the Co site of the  $\text{CoO}_2$  layers; in Na(2) it occupies the  $(2/3, 1/3, 1/4)$  lattice point above the center of the triangular lattice of the  $\text{CoO}_2$  layers; the third site Na(2)' is similar to the Na(2) one but  $\text{Na}^+$  is at  $(2x, x, 1/4)$ . The occupation probability of the above sites depends on both  $x$  and  $T$ . For  $x=0.5$  the  $\text{Na}^+$  ions are already arranged at room temperature in a periodic structure, both along the  $ab$  plane and the  $c$  axis, with Na(1) and Na(2) equally likely. At low  $T$ ,  $\text{Na}_{0.5}\text{CoO}_2$  becomes a charge-order insulator. It has been suggested that, since the  $\text{Na}^+$  ions exert a strong unscreened potential on the  $\text{CoO}_2$  layers, in the  $x=0.5$  samples the charge-ordered state in the layers mirrors<sup>2,3</sup> the periodic structure of the out-of-plane  $\text{Na}^+$  ions.  $\text{Na}^+$  order has been observed also for  $x \neq 0.5$  and seems more stable for commensurate doping ( $x=1/3, 1/2, 2/3, 3/4, 1$ ).<sup>3</sup>

The competition between charge mobility, localization, and ordering, in addition to a doping-dependent magnetic behavior, makes the  $(x, T)$  phase diagram<sup>4</sup> of  $\text{Na}_x\text{CoO}_2$  nearly as rich as that of La-Ca manganites.<sup>5</sup> Theory<sup>6</sup> shows that  $\text{CoO}_2$  is a Mott-Hubbard insulator, whereas  $\text{NaCoO}_2$  should be a narrow-gap band insulator or a semiconductor. By increasingly adding  $\text{Na}^+$  vacancies from  $x=1$ , the elec-

tron ground state changes from a spin-density-wave (SDW) metal (for  $0.75 \leq x < 1$ ) to a Curie-Weiss metal (for  $x < 0.75$ ). For  $x < 0.5$  the metallic state is characterized by a more conventional Pauli paramagnetism. The two regions are separated by the above-described 0.5 system. Once intercalated with water molecules, NCO becomes superconducting below about 5 K for  $1/4 < x < 1/3$ . The critical temperature  $T_c$  (Refs. 2 and 7) of  $\text{Na}_x\text{CoO}_2 \cdot y\text{H}_2\text{O}$  depends on  $y$ , also because the intercalated  $\text{H}_3\text{O}^+$  ions are likely to provide additional doping to the  $\text{CoO}_2$  planes.<sup>7</sup>

The low-energy excitations of the  $\text{CoO}_2$  plane have been studied by angle-resolved photoemission spectroscopy (ARPES) and infrared spectroscopy. ARPES detected, at  $x=0.7$ , a large hexagonal, hole-type, Fermi surface and a strongly renormalized quasiparticle band. This latter crosses the Fermi level in the  $\mathbf{k}$ -space direction from  $M$  to  $\Gamma$ . This corresponds to a single-particle hopping rate of 8 meV, consistently with the absence of quasifree particles at high  $T$ .<sup>8</sup>

Infrared spectra of  $\text{Na}_x\text{CoO}_2$  have been reported by several groups for different  $x$ .<sup>9-13</sup> A strong electron-phonon interaction and an anomalous Drude behavior have been found in  $x=0.57$  single crystals, where the charge carriers have an effective mass of about 5 electron masses and their scattering rate  $\Gamma(\omega)$  shows an  $\omega^{3/2}$  dependence.<sup>9</sup> Similar results have been found for  $x=0.7$ , a sample close to a SDW instability.<sup>10</sup> At  $x=0.5$ , the charge order shows up in the optical conductivity  $\sigma(\omega)$  through the opening of a gap at low temperature around  $150 \text{ cm}^{-1}$ .<sup>11,13</sup> Meanwhile, a far-infrared peak (FIP) springs up at  $200 \text{ cm}^{-1}$ , through a transfer of spectral weight (SW) across the gap.

However, an extended infrared study of charge localization and ordering in the  $(x, T)$  phase diagram of NCO has not been published yet. Here we study the in-plane infrared conductivity  $\sigma(\omega)$  of six single crystals of  $\text{Na}_x\text{CoO}_2$  covering the range  $0.5 \leq x \leq 1.0$ . In this whole range, the carriers are shown to be close to strong instabilities, leading to localization and ordering. These phenomena show up through a

strong FIP which at 0.5 is associated with a far-infrared gap. For  $x \geq 0.75$  the FIP is softer and coexists with a weak Drude term, while no gap is detected. A dramatic shift of the FIP to higher energies is observed, at high incommensurate  $x$ , between 30 and 12 K. This should be the effect of the spin-density-wave transition reported to occur in similar samples at 22 K.<sup>4</sup> Finally, by studying the phonon linewidth, we also obtain interesting information on the relation between charge localization in the  $\text{CoO}_2$  planes and “freezing” of the out-of-plane  $\text{Na}^+$  ions.

## II. EXPERIMENT AND RESULTS

Single crystals of  $\text{Na}_x\text{CoO}_2$  ( $0.5 \leq x \leq 1.0$ ) have been grown by the floating-zone method in a four-mirror image furnace under an oxygen/argon atmosphere at 106 Pa.<sup>14</sup> The nominal Na concentrations were chosen to explore the whole high- $x$  part of the phase diagram:  $x=0.5, 0.75, 0.85, 0.95, 1$ . After cutting the crystals, their real chemical composition was controlled by electron probe microanalysis (EPMA) on different points of the surface and resulted to vary within a 5% interval, which included the nominal value. The reflectivity  $R(\omega)$  of the six single crystals has been measured at quasnormal incidence ( $8^\circ$ ) between 320 and 8 K for  $40 < \omega < 20\,000 \text{ cm}^{-1}$ , by using a Michelson interferometer and with radiation polarized along the  $\text{CoO}_2$  layers. The final alignment of the reflectivity setup has been performed with the interferometer under vacuum by using remotely controlled motors to recover the mechanical stress of the optics due to interferometer evacuation. The crystals have been cleaved before each measurement to obtain a fresh and shiny surface. The reference was obtained by evaporating a gold or silver film, depending on the frequency range, onto the sample via a hot filament placed in front of it.

The reflectivity is shown at different temperatures in Fig. 1. That of the  $x=0.57$  sample<sup>15</sup> has been already published.<sup>9</sup> At room temperature,  $R(\omega)$  shows, for any Na content, an overall metal-like behavior, indicated by its increase for decreasing frequencies. The dependence of  $R(\omega)$  on doping is weak, consistently with the behavior of the resistivity, which for example varies by just a factor of 2 at 150 K between  $x=0.31$  and  $x=0.75$ ,<sup>4</sup> if one excludes the insulating system  $x=0.50$ . A pseudoplasma edge is also evident around  $5000 \text{ cm}^{-1}$ , for any  $x$  but 0.5, independently of the nominal doping. A similar effect has been observed in high- $T_c$  cuprates. Therein, the pseudoplasma edge could hardly be attributed to free-carrier absorption, like for the plasma edge of conventional metals. It was instead explained by an additional term centered in the midinfrared, having both peak frequency and intensity roughly independent of doping.<sup>16</sup> At  $x=0.5$ , on the other hand [Fig. 1(a)], the pseudoplasma edge is smeared compared to the other samples. Correspondingly, a lower value of the reflectivity is observed in the far- and midinfrared range at all temperatures.

As  $T$  decreases,  $R(\omega)$  monotonously increases below  $1500 \text{ cm}^{-1}$  in the  $x=0.57, 0.75$ , and 1 samples [Figs. 1(b), 1(c), and 1(f) respectively], through a transfer of spectral weight across that frequency. In the 0.5, 0.85, and 0.95 crystals instead [Figs. 1(a), 1(d), and 1(e), respectively], high-

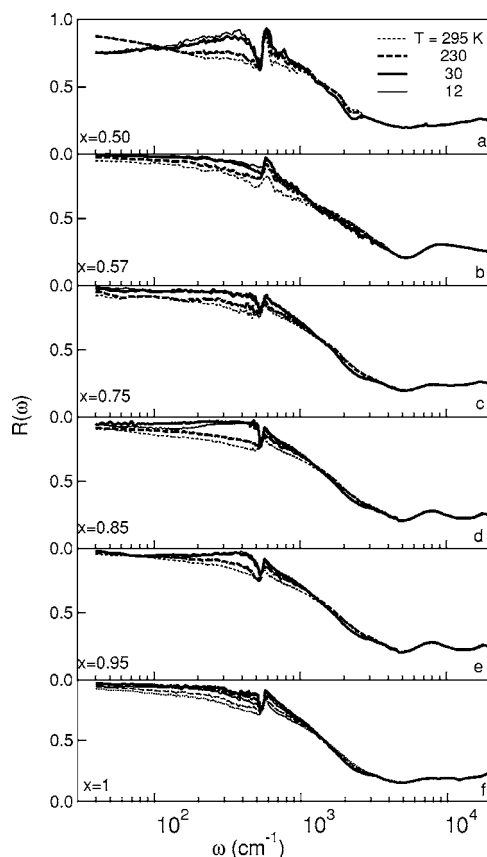


FIG. 1. In-plane infrared reflectivity of  $\text{Na}_x\text{CoO}_2$  for  $0.5 \leq x \leq 1$ , at different temperatures. For the sample with  $x=0.57$ , the lowest two temperatures are 90 and 20 K.

frequency spectral weight is transferred mainly to a bump around  $400 \text{ cm}^{-1}$ . A shallow minimum appears in  $R(\omega)$  around  $150 \text{ cm}^{-1}$ . At lower frequencies the reflectivity increases again to 1. All samples show a strong phonon absorption around  $590 \text{ cm}^{-1}$ . This corresponds to a “layer-sliding”  $E_{1u}$  mode related to the hexagonal  $P6_3/mmc$  structure, which results from the in-plane Co-O stretching motion mixed with a small component of the Na vibration parallel to the plane.<sup>17</sup> The other infrared-active phonon mode, predicted at about  $200 \text{ cm}^{-1}$ , is not observed. At high energy, the band peaked at  $8000 \text{ cm}^{-1}$  has been attributed to a charge-transfer transition between the  $2p$  O states and the  $3d$  Co electronic states, while that around  $15\,000 \text{ cm}^{-1}$  to a  $3d$ - $3d$  transition activated by a weak hybridization between  $3d$  Co and  $2p$  O states.<sup>9–11</sup> In the reflectivity of samples with  $x=0.5$  and 1 those two bands appear much broader and barely discernible. They are more clearly seen, even if not well resolved, in the resulting  $\sigma(\omega)$  (see Fig. 2).

The optical conductivity  $\sigma(\omega)$  was obtained from  $R(\omega)$  through standard Kramers-Kronig transformations.  $R(\omega)$  was extrapolated to zero frequency by using a standard Hagen-Rubens behavior and, at high frequencies, by a Lorentzian fit. An alternative high-frequency extrapolation based on the reflectivity<sup>18</sup> of  $\text{NdCoO}_3$  gave the same results within errors. The results are shown in Fig. 2 for all samples, at selected temperatures. It exhibits a strong temperature dependence up to  $800 \text{ cm}^{-1}$ , while its low-frequency behavior is certainly

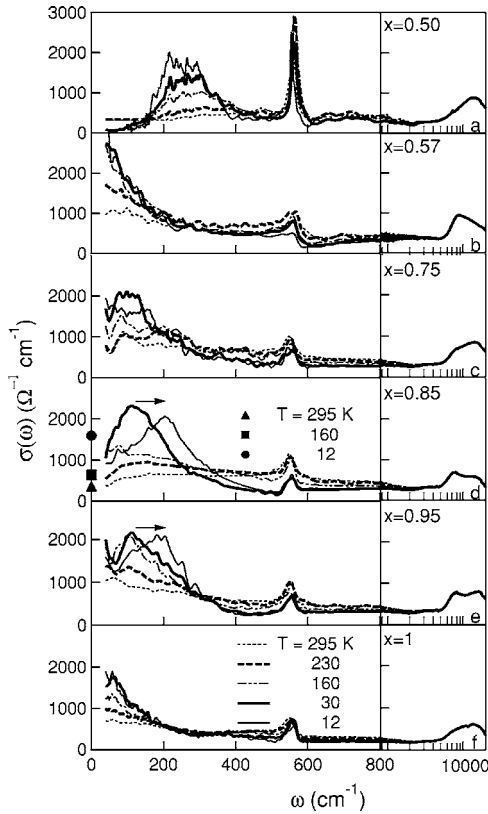


FIG. 2. Real part of the infrared conductivity of  $\text{Na}_x\text{CoO}_2$  for  $0.5 \leq x \leq 1$ , at different temperatures. For the sample with  $x=0.57$ , the lowest two temperatures are 90 and 20 K. The arrows mark the strong displacement below 30 K of the FIP in both samples with high and incommensurate doping ( $x=0.85, 0.95$ ). For  $x=0.85$ , dc conductivity values measured on the same sample are reported at three selected temperatures.

nonmonotonous versus  $x$ . At  $x=0.50$  [Fig. 2(a)] an overdamped FIP is centered around  $400 \text{ cm}^{-1}$  both at 295 and 230 K. Below that frequency a flat background is present, indicating incoherent charge transport at high temperature in the  $\text{CoO}_2$  layers. The peak increases in intensity by decreasing  $T$ . Between 230 and 160 K, the transfer of spectral weight from the in-gap states towards the peak opens a gap in the far-infrared  $\sigma(\omega)$  around  $150 \text{ cm}^{-1}$ , in agreement with the results of Refs. 11 and 13. At low  $T$  a peak at the same energy as here is evident in Ref. 13, even if upon heating it has a different temperature dependence. The  $x=0.57$  sample [Fig. 2(b)], the only one exhibiting a metal-like behavior, was extensively discussed in Ref. 9.

On the other hand, for  $x \geq 0.75$ , the far-infrared  $\sigma(\omega)$  looks like a combination of those for the charge-ordered 0.5 and the metallic 0.57 samples. At  $x=0.75$  a broad absorption peak is centered around  $200 \text{ cm}^{-1}$  at room temperature. Its intensity increases by lowering  $T$  down to 30 K, whereas its characteristic frequency shifts to about  $100 \text{ cm}^{-1}$ . However, both at 12 and 8 K [the latter one is not shown in Fig. 2(c) for the sake of clarity] spectral weight is lost below  $100 \text{ cm}^{-1}$  and transferred to higher frequencies. This effect is amplified both in the  $x=0.85$  and 0.95 samples [Figs. 2(d) and 2(e), respectively]. Therein a strong FIP develops at nearly

$100 \text{ cm}^{-1}$  below about 160 K and shifts to  $200 \text{ cm}^{-1}$  below 30 K. One may notice that, below 22 K, a SDW instability has been reported for  $0.7 \leq x \leq 0.9$ .<sup>4,19</sup> The FIP peak is separated from the quasiparticle contribution, clearly visible for the  $x=0.75$  and 0.95 samples below 50 and  $80 \text{ cm}^{-1}$ , respectively, by a minimum similar to that previously reported<sup>20</sup> at low  $T$  in a sample with  $x=0.7$ . In the  $x=0.85$  conductivity we could not resolve a Drude term from the FIP at low  $T$ . Therefore we measured the  $\rho(T)$  of this sample, which decreases linearly from 300 to 30 K; then, it increases smoothly. Its absolute values are in good agreement with those reported for  $x=0.82$  in Ref. 21. For clarity, in Fig. 2(d) we have reported only three  $\rho$  values at temperatures corresponding to those of selected  $\sigma(\omega)$  curves. At high  $T$ ,  $\rho(T)$  is in good agreement with the extrapolation of  $\sigma$  to  $\omega=0$ . At low  $T$  in the presence of a strong FIP, the dc value is higher than the extrapolated one, showing that a narrow Drude term does exist. It must be partly at frequencies below the limit of our data, partly hidden by the FIP.

Finally the nominally  $x=1$  sample, at variance with the theoretical predictions,<sup>6</sup> shows a metallic  $\sigma(\omega)$  that, at low frequencies, increases by lowering  $T$ . However, this unexpected behavior will be explained in the next section by the possible presence of a few Na defects in the nominally  $x=1$  crystal.

### III. DISCUSSION

#### A. Electronic conductivity

An FIP at finite energy associated with an optical gap, as in the present and previously reported<sup>11,13</sup>  $\sigma(\omega)$  of the  $x=0.5$  sample, is usually observed in the infrared conductivity of charge-ordered materials.<sup>22,23</sup> According to the charge-density-wave (CDW) theory,<sup>22,23</sup> the optical gap will measure the energy needed to excite one charge from its superlattice state (in  $\text{Na}_x\text{CoO}_2$ , the  $\text{Co}^{3+}$ - $\text{Co}^{4+}$  periodic structure) to  $E_F$ . In turn, a FIP in  $\sigma(\omega)$ , in the absence of full gap opening, in general reflects a coexistence of localized charges, not necessarily long-range ordered, and itinerant carriers. In this case, as it happens here for the samples with  $x=0.75$  and 0.95, a minimum separating the Drude term from the localization peak may appear in the optical conductivity. The energy of the FIP is that required to extract one charge from its potential well in an adiabatic (Frank-Condon) absorption process. The free carriers and the localized charges may be concentrated in different zones (phase separation) or not. The present infrared experiment cannot distinguish between such alternatives.

At  $x=0.5$  the energy gap here is on the order of  $150 \text{ cm}^{-1}$ , to be compared with the  $800$ – $1000 \text{ cm}^{-1}$  found in the charge-stripe state of the layered perovskite  $\text{La}_{1.33}\text{Sr}_{0.67}\text{NiO}_4$ .<sup>24,25</sup> This shows that charge ordering in  $\text{Na}_{0.5}\text{CoO}_2$  affects smaller energy regions around  $E_F$ . However, the strong depression of  $\sigma(\omega)$  below  $150 \text{ cm}^{-1}$  is consistent with the presence of a gap over the entire Fermi surface. The samples with  $x=0.75$  (Ref. 4), 0.85 (see below), and 0.95 (Ref. 26) show a metallic dc conductivity down to the lowest temperatures. However, as already mentioned,

$\sigma(\omega)$  shows at  $x=0.75$  [Fig. 2(c)] a minimum around  $50 \text{ cm}^{-1}$ , which deepens by lowering  $T$ . A similar minimum [Fig. 2(e)] appears around  $80 \text{ cm}^{-1}$  in the  $x=0.95$  sample. Both these minima separate a quasifree particle term from a FIP at about  $100 \text{ cm}^{-1}$ , as observed in certain cuprates.<sup>27</sup> This FIP is much softer than the corresponding one for the  $x=0.5$  sample, but shows a similar temperature dependence. Both at  $x=0.75$  and  $0.95$  the periodicity of magnetic correlations, measured by magnetic neutron scattering,<sup>28,29</sup> should rule out the occurrence of long-range  $\text{Co}^{3+}$ - $\text{Co}^{4+}$  order in these samples. Therefore the soft FIP can be assigned to localized charges, either disordered or with short-range order, coexisting with itinerant carriers in the  $\text{CoO}_2$  layers.

A clear shift to higher frequencies is observed in the FIP when  $T$  is lowered from 30 K to 12 K (data at 8 K, virtually superimposed to those at 12 K, have not been reported): the FIP displaces to about 120, 200, and  $200 \text{ cm}^{-1}$  for  $x=0.75$ , 0.85, and 0.95, respectively. That shift indicates a deepening of the localizing potential, through a further mechanism which takes place for the high-doping materials below 30 K. Between 30 and 12 K, moreover, a Drude-Lorentz fit to  $\sigma(\omega)$  shows that the quasiparticle term loses about 60% of its SW, for both  $x=0.75$  and 0.95. At  $x=0.85$ , instead, the Drude term is not resolved down to  $40 \text{ cm}^{-1}$ . Since this material shows a metallic dc conductivity at low  $T$ ,<sup>2</sup> one may infer that here the Drude term is weak and squeezed at very low frequencies.

The above strong effects on the low-energy charge dynamics at low  $T$  show that the SDW transition at  $T_{SDW} = 22 \text{ K}$  (Refs. 4 and 19) further gaps the Fermi surface. From the FIP shift one can estimate for the charges an additional binding energy  $E_{SDW}$  of about  $100 \text{ cm}^{-1}$ . This value is comparable with that measured for the SDW of Bechgaard salts  $(\text{TMTSF})_2X$  ( $X=\text{PF}_6, \text{ClO}_4$ ).<sup>23</sup> One thus obtains  $E_{SDW}/k_B T_{SDW} \sim 6$ , a value consistent with a strong-coupling spin-density wave. Moreover,  $E_{SDW}$  is of the same order as both the in-layer and  $c$ -axis magnetic exchange interactions which characterize the A-type antiferromagnetic structure.<sup>28,29</sup> Therefore the shift to higher energy of the FIP peak, below  $T_{SDW}$ , may be due to a strong interaction of the charge carriers with the in-layer ferromagnetically ordered spins. On the other hand, in the  $x=0.5$  material, the FIP frequency monotonously decreases down to 8 K, indicating the absence of any SDW instability in this system. Therefore, either the charge ordering showed by the 0.5 system on the charge localization in the  $x=0.75$ , 0.85, and 0.95 samples above 30 K must be due to a physical mechanism other than the SDW instability, which may be correlated both to the pinning potential of the out-of-plane  $\text{Na}^+$  ions and to the Hubbard repulsion between charge carriers in the  $\text{CoO}_2$  layers.

Finally,  $\sigma(\omega)$  at  $x=1$  unexpectedly does not show an insulating behavior, as instead predicted by band theory,<sup>6</sup> but is poorly metallic and increases by lowering  $T$  [Fig. 2(f)]. A FIP also appears at the lowest frequencies, between 200 and 160 K. These observations may be explained with a small number of  $\text{Na}^+$  vacancies, which introduce holes in the otherwise full  $e_{1g}$ - $a_g$  electronic bands. Indeed the SW of the  $x=1$  sample, obtained by integrating  $\sigma(\omega)$  up to the pseudo-plasma edge ( $\omega=5000 \text{ cm}^{-1}$ ), is about 40% of the corre-

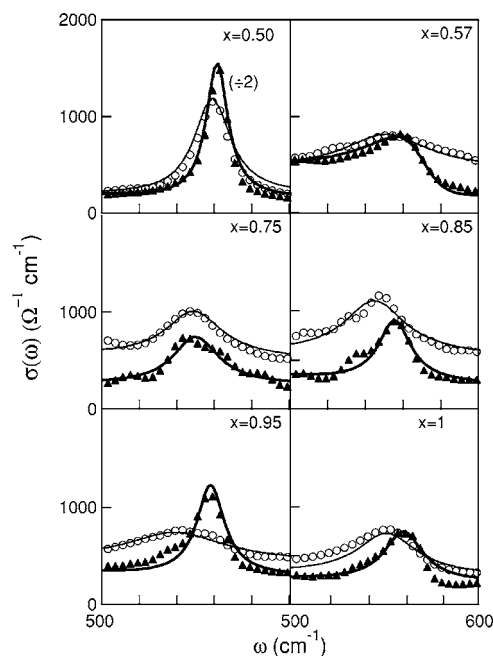


FIG. 3. Real part of the infrared conductivity corresponding to the  $E_{1u}$  in-plane phonon at 295 (open symbols) and 70 K (solid symbols). Thin and thick solid lines are Drude-Lorentz fits to data for 295 and 70 K, respectively (see text).

sponding SW at  $x=0.95$ . Assuming that the holes are only due to Na doping, the actual  $\text{Na}^+$  content of the nominally  $x=1$  sample can be estimated from the ratio  $\text{SW}(x=1)/\text{SW}(x=0.95)$  to be 0.98.

## B. Phonon absorption

Several authors have attributed the origin of charge ordering in  $\text{Na}_x\text{CoO}_2$  to the out-of-plane ordering of the  $\text{Na}^+$  ions.<sup>2,7</sup> Indeed, their partially screened Coulomb potential may affect the mobility of the charge carriers in the  $\text{CoO}_2$  layers. The “freezing” of the  $\text{Na}^+$  lattice below a certain temperature would favor a pinning of the charge carriers. One may not expect any direct observation of  $\text{Na}^+$  ordering in the infrared. However, as discussed in the Introduction, the “layer sliding”  $E_{1u}$  phonon mode [well evident in the  $\sigma(\omega)$  of all samples around  $590 \text{ cm}^{-1}$ ; see Fig. 2] contains a small component of the  $\text{Na}^+$  vibration parallel to the plane.<sup>17</sup> Therefore, the lifetime of this mode may be sensitive to ordering phenomena at the  $\text{Na}^+$  sites.

Figure 3 shows that this is indeed the case. Therein,  $\sigma(\omega)$  is reported for the six samples at two temperatures in the  $E_{1u}$  region ( $500\text{--}600 \text{ cm}^{-1}$ ), together with the Drude-Lorentz fit mentioned above. This latter provides the phonon parameters: intensity  $S_{ph}^2$ , frequency  $\omega_{ph}$ , and broadening  $\Gamma_{ph}$ . The results are rather accurate as the vibrational absorption, at any  $x$ , is well distinguished from the electronic background.

The resulting line width  $\Gamma_{ph}(T)$  is shown in Fig. 4 (left panels) as a function of  $T$  and  $x$ . One may notice that the  $T$  dependence of  $\Gamma_{ph}(T)$  is stronger for the incommensurate doping levels  $x=0.57$ , 0.85, and 0.95 than for the commensurate values. Several effects may influence the phonon

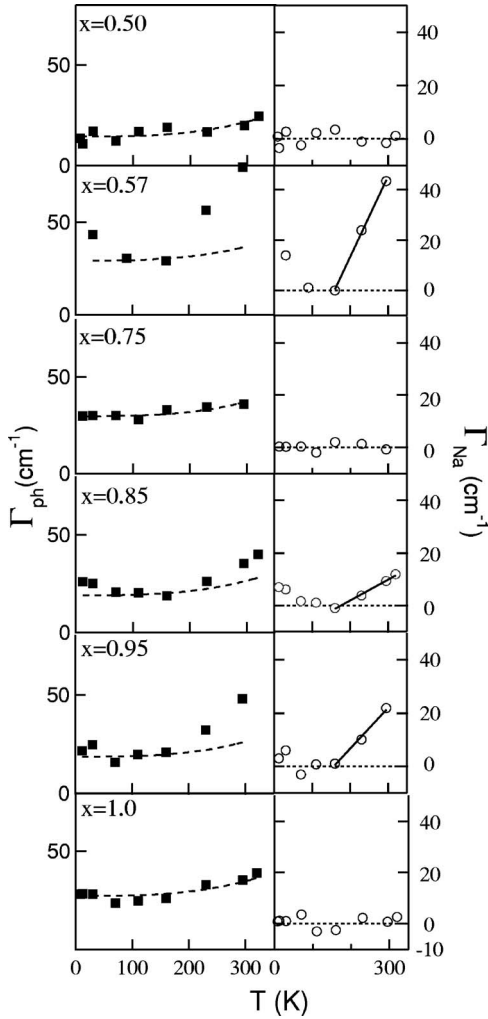


FIG. 4. Temperature dependence of the  $E_{1u}$  phonon broadening  $\Gamma_{ph}(T)$  (left panels, solid symbols), and its fit (dashed lines) to Eq. (2) (see text). In the right panels an estimate of  $\Gamma_{Na}(T)$  [see Eq. (1)] to the phonon broadening  $\Gamma_{ph}(T)$  is shown for all samples. Here the solid line is just a guide to the eye.

broadening: disorder in the  $\text{CoO}_2$  layers, inharmonic phonon-phonon interactions, and disorder in the  $\text{Na}^+$  lattice. Both last terms depend on  $T$ . Assuming that different decay channels are independent of each other, the phonon linewidth can be written as

$$\Gamma_{ph}(T) = \Gamma_0 + \Gamma_{ph-ph}(T) + \Gamma_{Na}(T), \quad (1)$$

where  $\Gamma_0$  is the contribution of structural disorder, both in the  $\text{CoO}_2$  layers and in the  $\text{Na}^+$  lattice,  $\Gamma_{ph-ph}(T)$  is due to the inharmonic phonon-phonon interaction, and  $\Gamma_{Na}(T)$  is related to thermal disorder and diffusion in the  $\text{Na}^+$  lattice. Also in oxides  $\Gamma_{ph-ph}(T)$  is well described by the usual law<sup>30</sup>  $a(T/\Theta)^3$ , where  $a$  is a constant and  $\Theta$  is the Debye temperature. If we assume, according to diffraction results, that in samples with commensurate doping, or near to it ( $x=0.5$ ,  $0.75$ , and  $1.0$ ) the  $\text{Na}^+$  ions are already frozen at room temperature,  $\Gamma_{Na}(T)=0$ . Therefore, for those samples one has

$$\Gamma_{ph}(T) = \Gamma_0 + a(T/\Theta)^3. \quad (2)$$

Satisfactory fits to Eq. (2), shown by the dashed lines in the left panels of Fig. 4, can be obtained for all samples which are at commensurate doping (within the compositional uncertainty) by varying  $\Gamma_0$  only and using the same  $a/\Theta^3 = 3 \times 10^{-7} \text{ cm}^{-1} \text{ K}^{-3}$ . As  $\Theta \approx 380 \text{ K}$  (Ref. 31) should not depend appreciably on the Na content, one obtains an  $x$ -independent  $a = 15 \pm 4 \text{ cm}^{-1}$ . The fit also gives  $\Gamma_0 = 25 \pm 5 \text{ cm}^{-1}$  for all samples, but for  $x=0.5$  where  $\Gamma_0 = 10 \pm 2 \text{ cm}^{-1}$ . Such a narrow line is then associated with the long-range Na order characteristic of this sample and is also consistent with that extracted from thermal conductivity measurements.<sup>4</sup>

As shown in Fig. 4, at the incommensurate  $x=0.57$ ,  $0.85$ , and  $0.95$  one observes clear deviations from Eq. (2), especially above  $200 \text{ K}$ . In those samples,  $\text{Na}^+$  thermal disorder probably gives a contribution to  $\Gamma_{Na}(T)$  also below  $300 \text{ K}$ . Moreover, one may notice that the increase of  $\Gamma_{ph}$  below  $100 \text{ K}$  for  $x=0.57$  (and probably for  $x=0.85$  and  $0.95$ ) is due to a Fano interaction between this phonon mode and the quasiparticle continuum, as discussed in a previous paper.<sup>9</sup> Since  $\Gamma_{Na}(T)$  is not known, we cannot predict the temperature behavior of  $\Gamma_{ph}(T)$  in the incommensurate systems. However, therein a freezing temperature for  $\text{Na}^+$  diffusion can be determined by subtracting from the experimental  $\Gamma_{ph}(T)$  that given by Eq. (2), which holds for  $\Gamma_{Na}(T)=0$  (commensurate doping). The resulting  $\Gamma_{Na}(T)$  is shown by open symbols in the right panels of Fig. 4, where the solid lines are guides to the eye. Therein we also show the fit residual, which for commensurate samples is obviously zero. In Fig. 4,  $\Gamma_{Na}(T)$  vanishes around  $150 \text{ K}$  for all samples with incommensurate Na content. Such a freezing temperature is in qualitative agreement with the value ( $200 \text{ K}$ ) found by diffraction measurements in polycrystalline samples with  $x > 0.7$ .<sup>32</sup>

The present data also provide information on the interplay between the above-detected  $\text{Na}^+$  “freezing” and the signatures of charge localization in the infrared conductivity. The FIP already present at room temperature for commensurate doping ( $x=0.5$  and  $0.75$ ) develops between  $230$  and  $160 \text{ K}$  in the incommensurate systems with  $x=0.85$  and  $0.95$ . In the same samples and temperature range, as shown above, the phonon linewidth has an anomalous  $T$  dependence due to increasing localization of the  $\text{Na}^+$  ions. On the other hand, the FIP is not observed at all when the incommensurate doping is  $0.57$ , even if  $\text{Na}^+$  ions freeze at the same temperature as in the other two samples. It seems then that charge localization—and possibly short-range charge order—is driven by the freezing of out-of-plane  $\text{Na}^+$  when the Na concentration is high and the charges density is low ( $x=0.85$  and  $0.95$ ). This mechanism becomes much less efficient when the  $\text{Na}^+$  concentration is low and the charge density is high ( $x=0.57$ ).

#### IV. CONCLUSION

In conclusion, we have carried out a systematic study of the optical conductivity of the  $\text{Na}_x\text{CoO}_2$  system in the  $x \geq 0.5$  part of its phase diagram. It is confirmed that charge

ordering opens, at  $x=0.5$ , a far-infrared gap about  $150\text{ cm}^{-1}$  wide. As a result, a peak appears around  $200\text{ cm}^{-1}$ , which corresponds to the lowest energy for exciting one charge out of the  $\text{Co}^{3+}$ - $\text{Co}^{4+}$  ordered ground state. At  $x=0.75$ ,  $0.85$ , and  $0.95$ , the gap is partially filled by Drude conductivity. This is separated by a minimum from a far-infrared peak, centered at about  $100\text{ cm}^{-1}$  at  $30\text{ K}$ . This FIP provides evidence that charge localization (or short-range charge order) competes with transport, since metallic conduction is observed at low  $T$  also for  $x>0.5$ . Moreover, the magnetic ordering reported in the literature below  $30\text{ K}$  and attributed to a spin-density-wave instability induces, for incommensurate  $x=0.85$  and  $0.95$ , a strong renormalization of the charge dynamics in the  $\text{CoO}_2$  planes. Indeed the far-infrared peak hardens dramati-

cally below  $30\text{ K}$  (by about  $100\text{ cm}^{-1}$ ), pointing towards a strong coupling of the charge and spin degrees of freedom. In contrast with these results, the  $x=0.57$  sample shows a metallic conduction at each  $T$ , described by an anomalous Drude behavior in the far-infrared  $\sigma(\omega)$ .

We have also shown that a correlation exists between the far-infrared peak and the out-of-plane localization of  $\text{Na}^+$  ions, monitored by the  $E_{1u}$  infrared-active phonon lifetime. In particular, the temperature where the FIP develops in the infrared conductivity is in reasonable agreement with the  $\text{Na}^+$  freezing temperature, as extracted from the phonon line-width. This mechanism, however, appears to be effective only for low charge density and high  $\text{Na}^+$  concentration.

- 
- <sup>1</sup>K. Takada, H. Sakurai, E. Takayama-Muromachi, F. Izumi, R. A. Dilanian, and T. Sasaki, *Nature (London)* **422**, 53 (2003).
- <sup>2</sup>H. W. Zandbergen, M. L. Foo, Q. Xu, V. Kumar, and R. J. Cava, *Phys. Rev. B* **70**, 024101 (2004).
- <sup>3</sup>Q. Huang, M. L. Foo, R. A. Pascal, Jr., J. W. Lynn, B. H. Toby, T. He, H. W. Zandbergen, and R. J. Cava, *Phys. Rev. B* **70**, 184110 (2004).
- <sup>4</sup>M. L. Foo, Y. Wang, S. Watauchi, H. W. Zandbergen, Tao He, R. J. Cava, and N. P. Ong, *Phys. Rev. Lett.* **92**, 247001 (2004).
- <sup>5</sup>P. Schiffer, A. P. Ramirez, W. Bao, and S.-W. Cheong, *Phys. Rev. Lett.* **75**, 3336 (1995).
- <sup>6</sup>K. W. Lee, J. Kuneš, and W. E. Pickett, *Phys. Rev. B* **70**, 045104 (2004).
- <sup>7</sup>C. J. Milne, D. N. Argyriou, A. Chemseddine, N. Aliouane, J. Veira, S. Landsgesell, and D. Alber, *Phys. Rev. Lett.* **93**, 247007 (2004).
- <sup>8</sup>M. Z. Hasan, Y.-D. Chuang, D. Qian, Y. W. Li, Y. Kong, A. Kuprin, V. Fedorov, A. R. Kimmerling, E. Rotemberg, K. Rossnagel, Z. Hussain, H. Koh, N. S. Rogado, M. L. Foo, and R. J. Cava, *Phys. Rev. Lett.* **92**, 246402 (2004).
- <sup>9</sup>S. Lupi, M. Ortolani, and P. Calvani, *Phys. Rev. B* **69**, 180506(R) (2004).
- <sup>10</sup>G. Caimi, L. Degiorgi, H. Berger, N. Barisic, L. Forró, and F. Bussy, *Eur. Phys. J. B* **40**, 231 (2004).
- <sup>11</sup>N. L. Wang, D. Wu, G. Li, X. H. Chen, C. H. Wang, and X. G. Luo, *Phys. Rev. Lett.* **93**, 147403 (2004).
- <sup>12</sup>C. Bernhard, A. V. Boris, N. N. Kovaleva, G. Khaliullin, A. V. Pimenov, L. Yu, D. P. Chen, C. T. Lin, and B. Keimer, *Phys. Rev. Lett.* **93**, 167003 (2004).
- <sup>13</sup>J. Hwang, J. Yang, T. Timusk, and F. C. Chou, *Phys. Rev. B* **72**, 024549 (2005).
- <sup>14</sup>D. Prabhakaran, A. T. Boothroyd, R. Coldea, and N. R. Charnley, *J. Cryst. Growth* **271**, 74 (2004).
- <sup>15</sup>F. Rivadulla, J. S. Zhou, and J. B. Goodenough, *Phys. Rev. B* **68**, 075108 (2003).
- <sup>16</sup>P. Calvani, M. Capizzi, S. Lupi, P. Maselli, A. Paolone, and P. Roy, *Phys. Rev. B* **53**, 2756 (1996).
- <sup>17</sup>Z. Li, J. Yang, J. G. Hou, and Q. Zhu, *Phys. Rev. B* **70**, 144518 (2004).
- <sup>18</sup>I. Terasaki, T. Nakahashi, A. Maeda, and K. Uchinokura, *Phys. Rev. B* **43**, 551 (1991).
- <sup>19</sup>B. C. Sales, R. Jin, A. Affholter, P. Khalifah, G. M. Veith, and D. Mandrus, *Phys. Rev. B* **70**, 174419 (2004).
- <sup>20</sup>N. L. Wang, P. Zheng, D. Wu, Y. C. Ma, T. Xiang, R. Y. Jin, and D. Mandrus, *Phys. Rev. Lett.* **93**, 237007 (2004).
- <sup>21</sup>S. P. Bayrakci, C. Bernhard, D. P. Chen, B. Keimer, R. K. Kremer, P. Lemmens, C. T. Lin, C. Niedermayer, and J. Stremper, *Phys. Rev. B* **69**, 100410(R) (2004).
- <sup>22</sup>M. Dressel and G. Grüner, *Electrodynamics of Solids* (Cambridge University Press, Cambridge, England, 2002).
- <sup>23</sup>G. Grüner, *Density Waves in Solids* (Addison-Wesley, Reading, MA, 1994).
- <sup>24</sup>Yu. G. Pashkevich, V. A. Blinkin, V. P. Gnezdilov, V. V. Tsapenko, V. V. Eremenko, P. Lemmens, M. Fischer, M. Grove, G. Guntherodt, L. Degiorgi, P. Wachter, J. M. Tranquada, and D. J. Buttrey, *Phys. Rev. Lett.* **84**, 3919 (2000).
- <sup>25</sup>P. Calvani, A. Paolone, P. Dore, S. Lupi, P. Maselli, P. G. Medaglia, and S.-W. Cheong, *Phys. Rev. B* **54**, R9592 (1996).
- <sup>26</sup>M. Mikami, M. Yoshimura, Y. Mori, T. Sasaki, R. Funahashi, and M. Shikano, in *Proceedings of the 21st IEEE International Conference on Thermoelectrics* (Institute of Electrical and Electronics Engineers, New York, 2002), p. 223.
- <sup>27</sup>S. Lupi, P. Calvani, M. Capizzi, and P. Roy, *Phys. Rev. B* **62**, 12418 (2000).
- <sup>28</sup>A. T. Boothroyd, R. Coldea, D. A. Tennant, D. Prabhakaran, L. M. Helme, and C. D. Frost, *Phys. Rev. Lett.* **92**, 197201 (2004); L. M. Helme, A. T. Boothroyd, R. Coldea, D. Prabhakaran, D. A. Tennant, A. Hiess and J. Kulda, *ibid.* **94**, 157206 (2005).
- <sup>29</sup>S. P. Bayrakci, I. Mirebeau, P. Bourges, Y. Sidis, M. Enderle, J. Mesot, D. P. Chen, C. T. Lin, and B. Keimer, *Phys. Rev. Lett.* **94**, 157205 (2005).
- <sup>30</sup>G. A. Thomas, D. H. Rapkine, S.-W. Cheong, and L. F. Schneemeyer, *Phys. Rev. B* **47**, 11369 (1993).
- <sup>31</sup>Y. Ando, N. Miyamoto, K. Segawa, T. Kawata, and I. Terasaki, *Phys. Rev. B* **60**, 10580 (1999).
- <sup>32</sup>Y. G. Shi, H. C. Yu, C. J. Nie, and J. Q. Li, cond-mat/0401052 (unpublished).